Surface Adsorbed Water on NaCl and Its Effect on Nitric Acid Reactivity with NaCl Powders

Sutapa Ghosal and John C. Hemminger*

Department of Chemistry, University of California, Irvine, Irvine, California 92697

Received: May 24, 2004

Adsorbed water has been shown to enhance the ionic mobility on NaCl surfaces at water vapor pressures well below the deliquescence point. This has important implications for the steady-state reactivity of NaCl, in atmospheric sea salt particles, with nitrogen oxides in the atmosphere. In the absence of surface ionic mobility the surface passivates due to the buildup of a product layer. It has also been suggested that the actual reaction probability of the reaction of HNO_3 with NaCl surfaces may depend on the water content of the surface. Using X-ray photoelectron spectroscopy and electron microscopy, we show that the specifics (particle size and water exposure) of the NaCl sample preparation can have significant effect on the amount of strongly adsorbed water (SAW) on the surface. Specifically, large single crystals of NaCl(100) do not adsorb water strongly. Crystallites in the size range of 500 μm adsorb small amounts of water strongly. In comparison, small crystallites in the size range of 1−10 μm can adsorb large amounts of water strongly. The strongly adsorbed water remains on the surface when exposed to vacuum at temperatures above 100 °C. The NaCl small crystallites, with the largest amount of strongly adsorbed water, do show a small increase in the initial reaction probability for the reaction with HNO_3. This increase in initial reaction probability is at most a factor of 4. By combining the results presented here with our previously reported quantitative measurement of the reaction probability for HNO_3 on NaCl(100) single-crystal surfaces we recommend a value of $\gamma = (5.2 \pm 3) \times 10^{-3}$ for the reaction probability of gaseous HNO_3 with micrometer-size NaCl particles that contain strongly adsorbed surface water.

Introduction

Reactive chlorine is extremely important to the chemistry of the troposphere. If generated in sufficient quantities, Cl atoms can significantly affect the tropospheric ozone balance and the oxidative capacity in the marine and coastal atmosphere.[6,7] In recent years, several field studies have reported the presence of various halogen species in the troposphere including Cl_2, BrCl, etc.[48,49,50] A major source of particulate Cl in the troposphere is sea salt aerosol, which is composed primarily of NaCl. Reactions of sea salt aerosol with the oxides of nitrogen (NO_y = HNO_3, N_2O_5, NO_2, $ClONO_2$) are known to generate gas-phase chlorinated products:[8−23]

$$HNO_3(g) + NaCl(s) \rightarrow NaNO_3(s) + HCl(g) \quad (1)$$

$$N_2O_5(g) + NaCl(s) \rightarrow NaNO_3(s) + ClNO_2(g) \quad (2)$$

$$2NO_2(g) + NaCl(s) \rightarrow NaNO_3(s) + ClNO(g) \quad (3)$$

$$ClONO_2(g) + NaCl(s) \rightarrow NaNO_3(s) + Cl_2(g) \quad (4)$$

As such, the deficit of Cl observed in sea salt particles in polluted air masses have been attributed to these reactions.[24−28] Compared to reactions 2−4, which form reactive chlorine-containing species, reaction 1 forms the relatively unreactive HCl. In order to estimate the reactive chlorine budget in the troposphere it is necessary to evaluate the relative importance of the various NO_y reactions with sea salt aerosol. In recent years there have been several field studies which report the presence of various halogen species in the troposphere.

The kinetics of reaction 1 has been investigated by several groups in an effort to determine its significance in the chemistry of the troposphere. While values of the reactive sticking coefficient (γ) for reaction 1 have been reported by various groups,[11,29−34,44,45,47] there are significant variations (spanning 2 orders of magnitude) in the reported data depending on the nature of the NaCl sample and the experimental conditions, in particular the HNO_3 pressure used in the experiment and the presence of adsorbed water.

We have shown previously that the dissociative adsorption of HNO_3 on NaCl is well described by a single-site Langmuir model.[44] In the absence of water, the mobility of surface ions is exceedingly low and the reaction saturates after the surface is coated with the nitrate product. Water-induced mobilization of the $NaNO_3$ reaction product is required to establish steady-state reaction conditions. Using this model[44] our data on NaCl(100) single-crystal surfaces predicts a maximum value for the reaction probability at zero product coverage (i.e., prior to surface passivation resulting from product buildup) of γ equal to $(1.3 \pm 0.6) \times 10^{-3}$. Values less than this maximum value are obtained by steady-state reaction experiments carried out under limited surface ionic mobility conditions (low surface water concentrations) where the reaction is limited by self-poisoning by the $NaNO_3$ reaction product. For instance, we have previously reported that the low reaction probability and the HNO_3 pressure dependent results of Davies and Cox[34] are due to self-poisoning of the surface reaction. Also, recently Hoffman et al.[47] have proposed a new model for reaction 1 that helps to

* Corresponding author. E-mail: jchemmin@uci.edu.

10.1021/jp047774c CCC: $27.50
Published on Web 08/24/2004

resolve much of the above-mentioned discrepancies and explain the larger values of γ that were reported by several groups based on experiments using NaCl crystallites under steady-state reaction conditions. Their model incorporates reactions at two different types of sites on the NaCl surface and proposes an overall average value of $\gamma = (1.0 + 0.8) \times 10^{-3}$.

As a result of the importance of water-enhanced ionic mobility to steady-state reaction conditions the role of adsorbed water in heterogeneous salt chemistry has been a topic of considerable interest. Experiments by several different groups have shown that the water content of the NaCl samples plays a critical role in the detailed mechanism of reaction 1. In the absence of adsorbed water the initial product of reaction 1 is a uniform, ultrathin, passivating $NaNO_3$ film, such that the reaction stops after only the first couple of layers of NaCl have reacted. However, water-induced mobilization of surface ions and the resultant reorganization of the $NaNO_3$ film have been shown to regenerate the NaCl surface for further reaction. Hemminger and co-workers[31,33] have reported the formation of microcrystallites of $NaNO_3$ upon exposure of the HNO_3-reacted NaCl surface to water vapor. Similar water-induced reorganization of the NaCl surface have been reported by Zangmeister et al.[43,45] based on their AFM observations of $NaNO_3$ "strings" along steps during the HNO_3−NaCl reaction. Also, Sporeleder et al.[46] present similar conclusions based on infrared spectroscopic studies of the same reaction. This reorganization of $NaNO_3$ at the surface exposes fresh NaCl surface for further reaction with HNO_3, thus allowing the reaction to proceed to the extent that ultimately a substantial portion of the Cl^- can be extracted from the NaCl particle. This is supported by field measurements whereby sea salt particles are known to have a Cl^- deficit relative to bulk seawater.[1−5,7,24,27]

Furthermore, the model presented by Hoffman et al.[47] proposes two different types of reaction sites: (1) steps and edges on the NaCl surface holding surface adsorbed water, and (2) dry terraces sites. According to their model, steps and edges on the NaCl surface are sites of continuous reaction due to the water-assisted regeneration of fresh NaCl surface at these locations. In contrast, the flat terrace sites, in the absence of adsorbed water, are saturated by the formation of a passivating $NaNO_3$ film. They attribute the initial rapid uptake of HNO_3 on NaCl, that they observe, to reaction with both types of sites on a fresh surface, followed by the slower, continuous uptake at the steps and edges at longer reaction times. In their model they assume that the initial reaction probability is the same for these two types of sites.

The water content of the NaCl surface is greatly influenced by the particular method of surface preparation and presentation.[36] There is evidence that surface defects lead to enhanced adsorption and dissociation of water on NaCl.[31,35,36] For instance, a freshly cleaved NaCl(100) single crystal is relatively defect-free, atomically smooth, and unreactive toward water vapor.[36] In contrast, ground powders and small crystallites tend to have a much higher density of edges, kinks, steps, and other surface defects, which can lead to chemisorption and dissociation of water to form surface OH^-.[35] The formation of surface OH^- is expected to further enhance water uptake by the surface, since owing to both the polarity and the formation of hydrogen bonds, water molecules are expected to cluster around surface OH^-. In their experiments, Beichert and Finlayson-Pitts[29] refer to this as strongly adsorbed water (SAW). Work of Ewing and co-workers on the adsorption of water on NaCl surfaces also confirms the enhanced dissociative adsorption of water on defective NaCl surfaces.[35−37]

On the basis of the work done in our laboratory and others, water adsorbed on NaCl surfaces may be broadly classified into the following three categories: (1) a liquid-like adlayer resembling saturated NaCl solution which is often referred to as a "quasi-liquid layer" and is observed even for water vapor pressures below the deliquescence point of NaCl, (2) trapped loosely bound water usually associated with loosely packed powder samples (this type of adsorbed water is typically removed from the surface upon gentle heating and evacuation of the sample chamber), and (3) strongly adsorbed water associated with defect sites which persists even after extensive exposure to low-humidity vacuum and requires aggressive heating for its removal.

In the work presented here we address two fundamental issues: first, the nature and content of surface adsorbed water on NaCl as a function of surface defects, and second, prior to the onset of saturation effects, is there a difference in the reaction probability of HNO_3 with NaCl with and without strongly adsorbed water. This second issue addresses whether the two kinds of sites involved in the reaction model presented by Hoffman et al.[47] should be considered to have the same initial reaction probabilities. To this end a variety of surface preparations have been considered, i.e., ground powders, small crystallites, and (100) single crystal. Furthermore, the effect of SAW on HNO_3 uptake has also been examined. Our results show that the surface water content on NaCl particles depends strongly on the particle size. The binding energy and the temperature dependence characteristics of the SAW-related oxygen signal on the NaCl samples are consistent with OH^- species. Unlike the (100) single crystal, the more defective surfaces show dissociative water uptake upon exposure to water vapor well below the deliquescence point of NaCl. According to the results we present here the presence of SAW on NaCl increases the reaction probability with HNO_3 by at most a factor of 4. On the basis of our results presented here we recommend a value of $\gamma = (5.2 \pm 3) \times 10^{-3}$ for the reaction probability for reaction 1 for small NaCl particles (1−10 μm) with strongly adsorbed surface water. This value is in good agreement with the new reaction model proposed by Hoffman et al.[47] for reaction 1. They report a value of $\gamma^\circ = (2.3 \pm 1.9) \times 10^{-3}$ for the initial uptake coefficient, which they associate with reaction on a fresh NaCl surface in the absence of a passivating nitrate product on the surface.

Experimental Section

X-ray photoelectron spectroscopy experiments have been carried out using a multitechnique ultrahigh vacuum (UHV) surface analysis instrument (VG Instruments ESCALAB MkII). The details of the instruments and the method of independently dosing HNO_3 and/or water on the NaCl samples have been described in detail previously.[38] Briefly, a 50:50 v/v solution of HNO_3 and H_2SO_4 was used as the source for dry, gaseous HNO_3 and an all-glass capillary doser was used for dosing. Mg Kα X-rays (1253.6 eV), Al Kα X-rays (1486.6 eV), and an analyzer pass energy of 20 eV were utilized for all the experiments.

NaCl(100) samples were prepared as thin wafers by cleavage from a rectangular single-crystal block. Powdered NaCl samples were produced by grinding single-crystal pieces in a ball mill, which generated particles with diameters in the 1−10 μm range. The powder was pressed into a tantalum mesh (∼1 cm diameter) welded to rhenium heating wire. The pressing was done at room temperature by placing the mesh and the powder between two stainless steel bolts such that both sides of the mesh were

covered by powder and then pressing them together on a bench press. A thermocouple was attached to the edge of the mesh. This provided a secure way to introduce powdered samples into the vacuum chamber and to heat and monitor the temperature of the sample. The small crystallites were obtained by sieving commercial NaCl powders (Fluka, >99.5%) and retaining the fraction that passed through a no. 20 sieve but not a no. 40 sieve. This gave particles with an average diameter of ~500 μm. The crystallites were pressed into a 1 cm × 1 cm piece of indium foil (Goodfellow, 99.999%) for introduction into the vacuum chamber. This arrangement did not allow for heating of the crystallites. All the samples were prepared under ambient conditions and promptly transferred to the UHV chamber for pump down to UHV conditions.

XPS peak areas for N, Cl, O, and Na were measured after standard Shirley-type background subtraction. Standard XPS sensitivity factors for N, O, and Cl (0.489, 0.745, 0.996, respectively, relative to the *F* sensitivity factor of 1.00) were used to quantify the surface concentrations of these elements.[39,40] The XPS sensitivity factor for Na is not well established in the literature, so we used a relative sensitivity factor of 3.8, developed for our instrument and experimental conditions, that gives a Na/Cl ratio of 1:1 for freshly cleaved, clean NaCl(100).[38]

Results and Discussion

Characterization of the NaCl Surface. Figure 1 shows SEM images of the three different types of NaCl samples used in these experiments. As is evident from Figure 1, different methods of sample preparation greatly influence the surface morphology of the salt. A freshly cleaved NaCl(100) surface is remarkably defect-free with smooth terraces. In contrast, the small crystallites and powdered samples, comprised of much smaller particles, have considerably more surface defects. The crystallite particle sizes used in our experiments are on the order of 500 μm, while the powder particle sizes we used are in the 1−10 μm range.

Surface Adsorbed Water. Figure 2 shows the O(1s) photoelectron spectra for the three different kinds of freshly prepared NaCl samples immediately after pump down to ultrahigh vacuum conditions. The O(1s) observed in our experiments on the 500 μm crystallites and powder samples (binding energy = 531.5 eV) is in the range of values expected for surface hydroxide species.[40] As is evident from Figure 2, powdered NaCl particles (~10 μm diameter) have significantly larger surface water content compared to either the small NaCl crystallites (~500 μm diameter) or the NaCl(100) single crystal. In fact no surface oxygen is detected for the single crystal suggesting that there is no surface adsorbed water on the NaCl(100) surface at room temperature under UHV conditions. This is consistent with the well-known fact that water does not dissociate on such low defect density NaCl surfaces and H_2O desorbs from these surfaces at temperatures well below room temperature under vacuum conditions.[36,41,42] In Figure 3 we show the O surface composition (relative to Na) for the three types of NaCl samples, providing a quantitative comparison of the surface water content on the three sample types. The spectra of the NaCl(100) surface show no residual oxygen following water exposure and subsequent pump down. In this figure the value indicated for NaCl(100) sample is indicative of the XPS sensitivity limit. It is clear that NaCl powdered samples with particle diameters of ≤500 μm contain substantial amounts of surface adsorbed water. Hence our results confirm the fact that defective surfaces lead to enhanced dissociative adsorption of water.

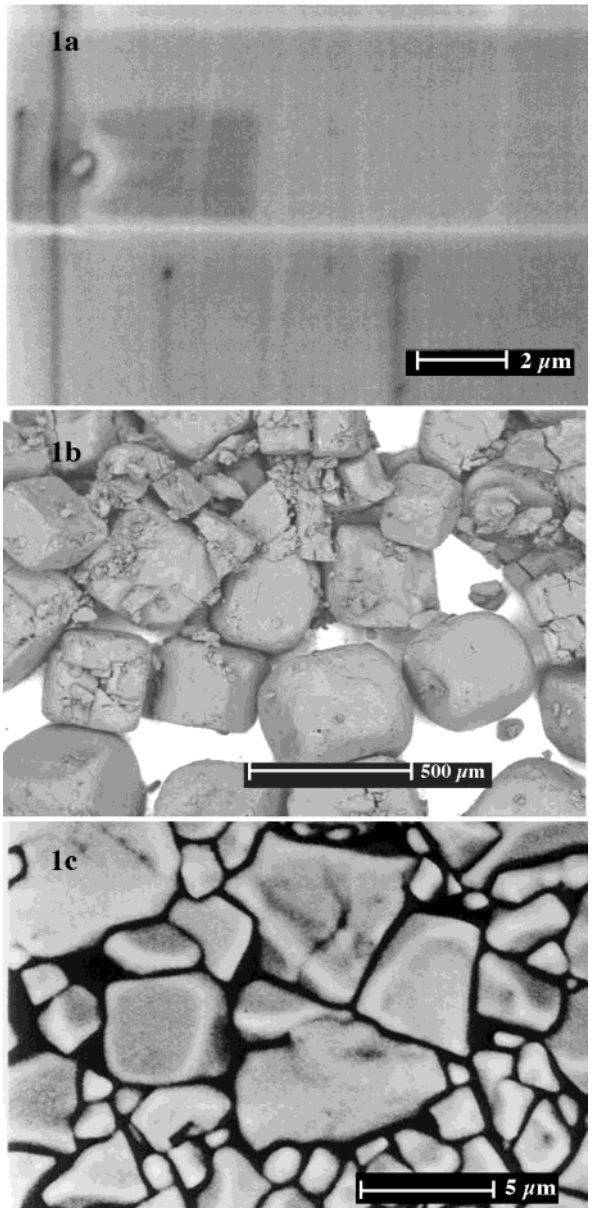

Figure 1. SEM images of the three different types of NaCl samples used in the experiments described here: (a) freshly cleaved NaCl(100) single-crystal surface; (b) small NaCl crystallites that are a few hundred micrometers on an edge; (c) ground powders of NaCl, that are 1−10 μm in diameter.

The dissociative water adsorption was further explored through experiments on water uptake by the powdered NaCl samples (1−10 μm diameter). Figure 4 shows a comparison of the O(1s) photoelectron spectra for the powdered sample following exposure to two different water vapor pressures. The water exposures were for 30 min in each case. Thus, the spectra shown in Figure 4 correspond to water exposures of 1.8×10^{10} Langmuir (10 Torr for 30 min) and 4.3×10^{10} Langmuir (24 Torr for 30 min). As was mentioned previously and is also evident in Figure 4, there is preexisting strongly adsorbed water on the freshly prepared powdered NaCl sample even prior to any water vapor exposure experiments. This strongly adsorbed water persists on the sample even after prolonged exposure to vacuum at room temperature. Buildup of this surface water is most likely initiated by water uptake during the sample preparation process under ambient conditions. Exposure to low pressures of water vapor under our experimental conditions leads to further buildup of strongly adsorbed water on the powdered

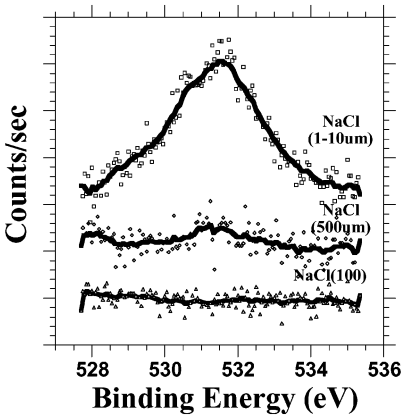

Figure 2. O(1s) photoelectron spectra for the three different kinds of freshly prepared NaCl samples used in these studies. The spectra were taken immediately following pump down to ultrahigh vacuum conditions.

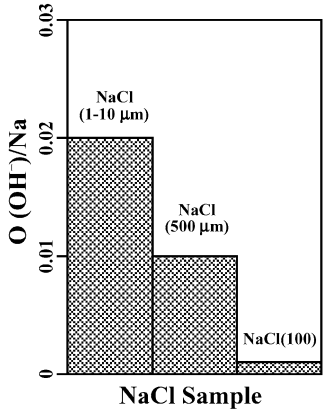

Figure 3. Oxygen surface composition (assumed to be present as OH^- due to the observed O(1s) binding energy) for the three different kinds of NaCl samples used in this study. The value shown for NaCl(100) single crystals is the XPS sensitivity limit since no oxygen is observed on this surface after pump down in our experiments.

sample. Exposure to water vapor at pressures above the deliquescence point of NaCl, such as the 24 Torr exposure shown in Figure 4, results in large amounts of residual adsorbed water that shows an oxygen binding energy of 532 eV which is more characteristic of molecular water. However, as can be seen in the figure, buildup of surface adsorbed water on the powdered sample is observed even for water vapor exposure at a pressure (e.g., 10 Torr) below the deliquescence point of NaCl.

Water uptake on the powdered sample was also studied under conditions where the freshly prepared sample was heated (in vacuum) prior to water vapor exposure in order to remove the preexisting SAW from the surface. The buildup of SAW on the powdered sample with continuing water vapor exposure under our experimental conditions is depicted in Figure 5 where we plot the surface O composition (relative to Na) as a function of water vapor exposure at 13 Torr. As is evident from the figure, water uptake by the powdered sample continues even for long exposure times. This is in contrast to the behavior reported for freshly cleaved NaCl(100) single crystals which show no detectable presence of adsorbed water after returning the samples to UHV conditions following substantial exposure to water vapor.[31] The water uptake behavior of powdered NaCl ($\sim$10 μm particle diameter) is consistent with the picture of a highly defective surface.

The temperature dependence of the strongly adsorbed water on the powdered NaCl particles ($\sim$10 μm diameter) was

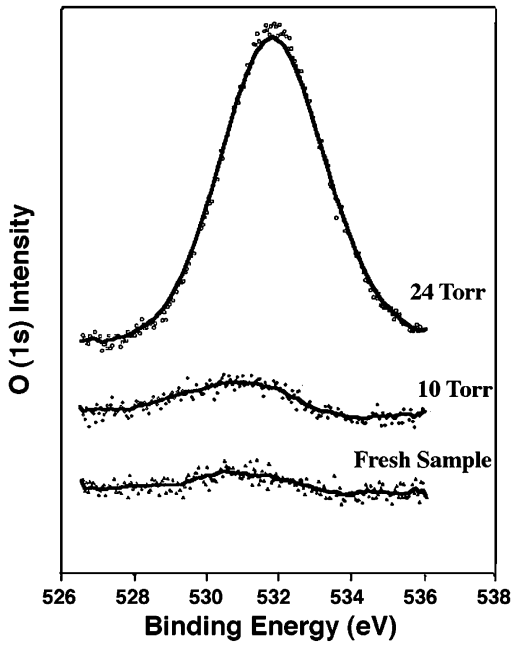

Figure 4. O(1s) photoelectron spectra for a powdered NaCl sample (1−10 μm diameter) following exposure to the following: no additional water; 10 Torr of water vapor for 30 min; and 24 Torr of water vapor for 30 min.

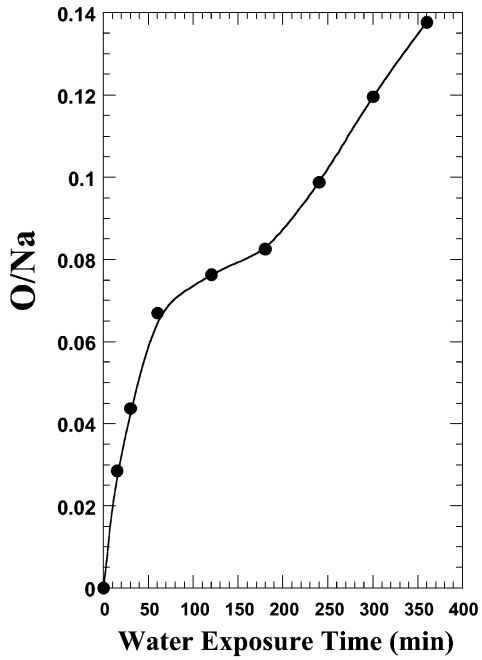

Figure 5. Surface O/Na ratio for powdered NaCl (1−10 μm diameter) as a function of water exposure time at 13 Torr of water vapor. The sample was heated in a vacuum prior to these experiments to remove any residual strongly adsorbed water from ambient exposure prior to placing the sample in the vacuum chamber.

investigated in an attempt to probe the nature of its bonding to the NaCl surface. The sample was sequentially annealed to the temperatures of interest under vacuum, and X-ray photoelectron spectra were collected after each annealing treatment to monitor changes in the surface composition. All spectra were collected with the sample at room temperature. Figure 6 shows a comparison of the O(1s) photoelectron spectra for the small NaCl particles following three different annealing temperatures. As is evident from the figure there is no obvious change in the surface O content of the sample for temperatures $\leq$100 °C.

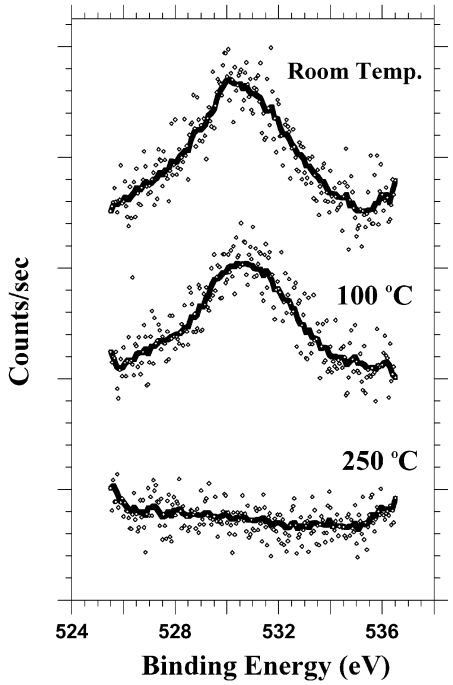

Figure 6. O(1s) photoelectron spectra for powdered NaCl (1−10 μm diameter) sample as a function of annealing temperature. The spectrum labeled as "room temp" is from a sample analyzed immediately after preparation under ambient air condition. The spectra were obtained with the sample at room temperature after annealing to the indicated temperature.

However, following heating to 250 °C the O signal is no longer detectable. This demonstrates that there is significant loss of surface adsorbed water in the 100−250 °C temperature range. Hence the strongly adsorbed water is stable on the surface up to temperatures of at least 100 °C.

Reaction with HNO_3. As was mentioned in the Introduction we are interested in determining if the presence of strongly adsorbed water on NaCl has a significant impact on its reaction with gaseous HNO_3 beyond the impact on the product ionic mobility that we have shown previously. In order to help elucidate the role played by SAW in the reaction of solid NaCl with gaseous HNO_3, we have studied the HNO_3 uptake characteristics of variously prepared NaCl samples. Since, as we have just discussed, the method of sample preparation has a strong influence on the water content of the NaCl sample, differently prepared samples have different amounts of SAW. The various NaCl samples studied in our experiments are (1) NaCl(100) single crystal, (2) freshly prepared NaCl powder (∼10 μm diameter) (this sample contains small amounts of SAW from ambient exposure during sample preparation), (3) NaCl powder (∼ 10 μm diameter) preheated to remove residual SAW and, (4) preheated NaCl powder (∼10 μm diameter) which was subsequently exposed to a specific amount of water vapor to induce SAW buildup.

In these experiments, we follow the buildup of the $NaNO_3$ reaction product by monitoring the N(1s) photoelectron peak.[31−33] Figure 7, where we plot the surface N content (relative to Na) as a function of HNO_3(g) exposure, shows a comparison of the HNO_3 uptake by three differently treated NaCl powder (∼10 μm diameter) samples. The open squares represent a sample that was annealed prior to HNO_3 exposure to remove all residue of SAW from the surface (O/Na = 0.0); the open circles correspond to a freshly prepared sample that contained a small amount of SAW from ambient exposure (O/Na = 0.05); and finally the filled circles represent a sample that was first annealed

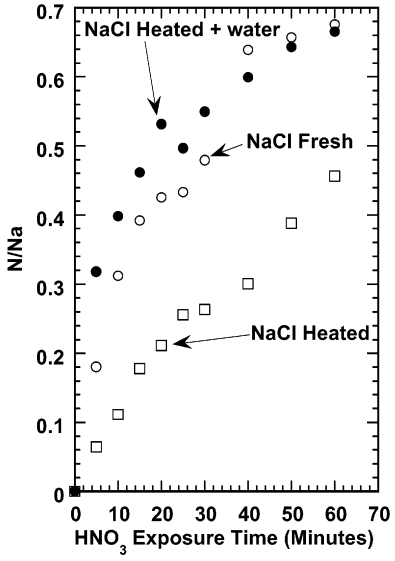

Figure 7. Surface $NaNO_3$ production (expressed by the N/Na surface ratio) for three powdered NaCl samples (1−10 μm diameter) as a function of gaseous HNO_3 exposure. Data for three different samples with different amounts of strongly adsorbed water are shown.

to remove all residual SAW followed by exposure to water vapor to initiate a large SAW buildup on the surface (O/Na = 1.0). Thus Figure 7 allows a comparison of the HNO_3 uptake on the NaCl powder (∼10 μm diameter) sample as a function of the SAW content of the sample.

Comparison between the two NaCl powder (∼10 μm diameter) samples with different amounts of SAW suggests that the exact amount of SAW on the surface has little overall impact on the kinetics of reaction 1; the most obvious effect is in the initial HNO_3 uptake which shows a slight enhancement in the presence of increased amount of SAW. This can be quantified by plotting the data of Figure 7 in the manner suggested by a Langmuir adsorption process ($-\ln(1 - ([\text{nitrate}]/[\text{nitrate}]_{max})$) versus HNO_3 exposure). Figure 8 shows Langmuir plots of the data from the samples with different SAW content (using the N(1s) XPS peak area (corrected for sensitivity factors) as the nitrate surface concentration). The high-quality linear least-squares fits to the three data sets indicate that the results are consistent with a Langmuir adsorption model. The slopes obtained from the plots in Figure 8 are proportional to the initial (zero coverage) reaction probability for HNO_3 on these surfaces. We do not report here an absolute number for the reaction probabilities, since this requires a detailed knowledge of the number of active sites available on the clean surface (surface area), which is not easily ascertained for these powdered samples. We can, however, compare the reaction probabilities for the 10 μm powdered samples with different amounts of SAW, since they all have the same surface areas. As can be seen from Figure 8, the reaction probability on the heated sample (no SAW) is slightly less than that on the samples with SAW. The two samples with low level and high level of SAW have identical reaction probability within our experimental precision. In the presence of SAW the reaction probability is greater by a factor of ∼4 as compared to the surface with no SAW. Thus while there is a small *initial* reactivity enhancement in the presence of SAW, the existence of SAW on the surface does not lead to a large enough increase in reactivity to explain the large values of γ reported in the literature.

From Figure 7 it apparent that even in the presence of SAW the reaction saturates. This is in contrast to the observations of Hoffman et al.[47] According to their model the surface would

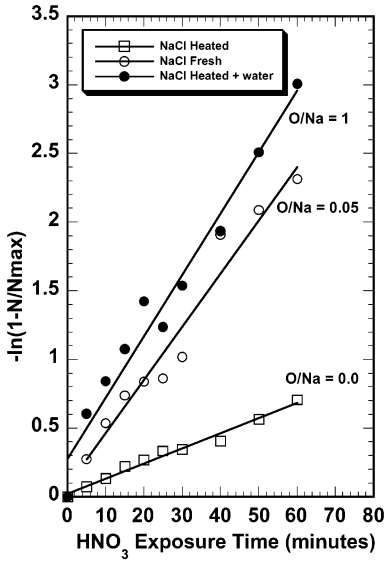

Figure 8. Langmuir plots ($-\ln(1 - ([\text{nitrate}]/[\text{nitrate}]_{max})$) vs HNO_3 exposure) for the dissociative adsorption of HNO_3 to form $NaNO_3$ on powdered NaCl samples (1−10 μm diameter) with different amounts of strongly adsorbed water. The strongly adsorbed water content of the surface is indicated by the O/Na ratio measured at the beginning of the experiment. The lines represent linear least-squares fits to the data points.

not become saturated as long as fresh NaCl steps continue to be generated in the presence of SAW. In their experiments, quantification was based on signals from gas-phase species, while in our case we monitored the formation of surface nitrate using XPS, which is only sensitive to the first few layers closest to the surface. Given the nitrate layer reorganizes and phase separates from the NaCl surface in the presence of SAW, it is likely that beyond a certain thickness of the phase-separated nitrate, the XPS technique is not sensitive to further nitrate formation. Thus, in our case the nitrate layer appears to saturate even though it is possible that nitrate continues to be formed in the presence of SAW.

As mentioned earlier it had been suggested that the presence of SAW on the NaCl surface may have a significant impact on the reactive uptake of gas-phase species by the surface and thus may help explain the inconsistencies between the reported values of γ for reaction 1 on different NaCl sample presentations. We do observe an increase in the surface reactivity in the presence of SAW, however, based on the results presented here the effect of SAW on the reactive uptake of HNO_3 by NaCl surfaces is not sufficient to explain reaction rates more than a factor of 4 larger than the value of $(1.3 \pm 0.6) \times 10^3$ that we have obtained for NaCl(100) single-crystal surfaces.[44] By combining our results reported here with our previous quantitative measurements of the reaction probability for HNO_3 with NaCl(100) single-crystal surfaces, the largest value we could obtain for the reaction probability for small particles with strongly adsorbed water would be ($\gamma = (5.2 \pm 3) \times 10^{-3}$).

In conclusion, our results support the model that defective surfaces lead to enhanced dissociative adsorption of water on the surface. Unlike the defect-free NaCl(100) single-crystal surface NaCl particles, both the small crystallites (~500 μm diameter) and the ground powder (~10 μm diameter) show dissociative water uptake upon exposure to water vapor pressure below the deliquescence point of NaCl. While our results confirm the existence of strongly adsorbed water on defective NaCl surfaces, SAW leads to at most a factor of 4 increase in the reaction probability for reaction 1. By combining the results we present here with our previously reported quantitative measurements of the reaction probability for reaction 1 on NaCl(100) single crystals we recommend the use of a reaction probability of $\gamma = (5.2 \pm 3) \times 10^{-3}$ for the reaction of gaseous HNO_3 with sea salt particles that likely contain significant amounts of strongly adsorbed water under typical ambient conditions in the troposphere.

Acknowledgment. This work was supported by National Science Foundation Grants, ATM 9707285 and ATM 0080806. We thank Professor B. J. Finlayson-Pitts and Dr. Koji Inazu for many helpful discussions regarding this work.

References and Notes

(1) Martens, C. S.; Wesolowski, J. J.; Harris, R. C.; Kaifer, R. J. *J. Geophys. Res.* **1973**, *78*, 8778.
(2) Duce, R. A.; Hoffman, E. J. *Annu. Rev. Earth Planet. Sci.* **1976**, *4*, 187.
(3) Kritz, M. A.; Rancher, J. J. *J. Geophys. Res.* **1980**, *85*, 1633.
(4) Parungo, F. P.; Nagamoto, C. T.; Madel, R.; Rosinski, J.; Haagenson, P. L. *J. Aerosol Sci.* **1987**, *18*, 277.
(5) Graedel, T. E.; Keene, W. C. *Global Biogeochem. Cycles* **1995**, *9*, 47.
(6) Finlayson-Pitts, B. J.; Pitts, J. N., Jr. *Upper and Lower Atmosphere: Theory, Experiments and Applications*; Academic Press: San Diego, 2000.
(7) Cicerone, R. J. *Rev. Geophys. Space Phys.* **1981**, *19*, 123.
(8) Schroeder, W. H.; Urone, P. *Environ. Sci. Technol.* **1974**, *8*, 756.
(9) Robbins, R. C.; Cadle, R. D.; Eckhardt, D. L. *J. Meteorol.* **1959**, *16*, 53.
(10) Cadle, R. D.; Robbins, R. C. *Discuss. Faraday Soc.* **1960**, *30*, 155.
(11) Leu, M. T.; Timonen, R. S.; Keyser, L. F.; Yung, Y. L. *J. Phys. Chem.* **1995**, *99*, 13203.
(12) Fenter, F. F.; Caloz, F.; Rossi, M. J. *J. Phys. Chem.* **1994**, *98*, 9801.
(13) Finlayson-Pitts, B. J.; Ezell, M. J.; Pitts, J. N., Jr. *Nature* **1989**, *337*, 241.
(14) Livingston, F. E.; Finlayson-Pitts, B. *J. Geophys. Res. Lett.* **1989**, *18*, 17.
(15) Behnke, W.; Scher, V.; Zetzsch, C. *J. Aerosol Sci.* **1993**, *24*, S115.
(16) George, Ch.; Ponche, J. L.; Mirabel, Ph.; Behnke, W.; Scher, V.; Zetzsch, C. *J. Phys. Chem.* **1994**, *98*, 8780.
(17) Msibi, I. M.; Li, Y.; Shi, J. P.; Harrison, R. M. *J. Atmos. Chem.* **1994**, *18*, 291.
(18) Finlayson-Pitts, B. J. *Nature* **1983**, *306*, 676.
(19) Vogt, R.; Finlayson-Pitts, B. J. *J. Phys. Chem.* **1994**, *98*, 3747; **1995**, *99*, 13052.
(20) Vogt, R.; Finlayson-Pitts, B. *J. Geophys. Res. Lett.* **1994**, *21*, 2291.
(21) Junkermann, W.; Ibusuki, T. *Atmos. Environ.* **1992**, *26A*, 3099.
(22) Winkler, T.; Goschnick, J.; Ache, H. J. *J. Aerosol Sci.* **1991**, *22*, S605.
(23) Timonen, R. S.; Chu, L. T.; Leu, M. T.; Keyser, L. F. *J. Phys. Chem.* **1994**, *98*, 9509.
(24) Junge, C. E. *Tellus* **1956**, *8*, 127.
(25) Moyers, J. L.; Duce, R. A. *J. Geophys. Res.* **1972**, *77*, 5330.
(26) Keene, W. C.; Pszenny, A. A. P.; Jacob, D. J.; Duce, R. A.; Galloway, J. N.; Schultz-Tokos, J. J.; Sievering, H.; Boatman, J. F. *Global Biogeochem. Cycles* **1990**, *4*, 407.
(27) Mouri, H.; Okada, K. *Geophys. Res. Lett.* **1993**, *20*, 49.
(28) McInnes, L. M.; Covert, D. S.; Quinn, P. K.; Germani, M. S. *J. Geophys. Res.* **1994**, *99*, 8257.
(29) Beichart, P.; Finlayson-Pitts, B. J. *J. Phys. Chem.* **1996**, *100*, 15218.
(30) Fenter, F. F.; Caloz, F.; Rossi, M. J. *J. Phys. Chem.* **1996**, *100*, 1008.
(31) Laux, J. M.; Fister, T. F.; Finlayson-Pitts, B. J.; Hemminger, J. C. *J. Phys. Chem.* **1996**, *100*, 19891.
(32) Laux, J. M.; Hemminger, J. C.; Finlayson-Pitts, B. *J. Geophys. Res. Lett.* **1994**, *21*, 1623.
(33) Allen, H. C.; Laux, J. M.; Vogt, R.; Finlayson-Pitts, B. J.; Hemminger, J. C. *J. Phys. Chem.* **1996**, *100*, 6371.
(34) Davies, J. A.; Cox, R. A. *J. Phys. Chem. A* **1998**, *102*, 7631.
(35) Dai, D. J.; Peters, S. J.; Ewing, G. E. *J. Phys. Chem.* **1995**, *99*, 10299.
(36) Ewing, G. E.; Peters, S. J. *Surf. Rev. Lett.* **1997**, *4*, 757.
(37) Peters, S. J.; Ewing, G. E. *J. Phys. Chem.* **1996**, *100*, 14093.
(38) Laux, J. M. X-ray Photoelectron Spectroscopy Studies of the Reaction of Nitric Acid and Sodium Chloride: Effects of Water, Surface

Defects and X-rays. Ph.D. Dissertation, University of California, Irvine, CA, 1996.

(39) Wagner, C. D.; Davis, L. E.; Zeller, M. V.; Taylor, J. A.; Raymond, R. H.; Gale, L. H. *Surf. Interface Anal.* **1987**, *3*, 211.

(40) Moulder, J. F.; Stickle, W. F.; Sobol, P. E.; Bomben, K. D. *Handbook of X-ray Photoelectron Spectroscopy*; Perkin-Elmer Corp., Physical Electronics Division: Eden Prairie, MN, 1992.

(41) Fölsch, S.; Henzler, M. *Surf. Sci.* **1991**, *247*, 269.

(42) Fölsch, S.; Stock, A.; Henzler, M. *Surf. Sci.* **1992**, *264*, 65.

(43) Zangmeister, C. D.; Pemberton, J. E. *J. Phys. Chem. B* **1998**, *102*, 8950.

(44) Ghosal, S.; Hemminger, J. C. *J. Phys. Chem. A* **1999**, *103*, 4777.

(45) Zangmeister, C. D.; Pemberton, J. E. *J. Phys. Chem. A* **2001**, *105*, 3788.

(46) Sporeleder, D.; Ewing, G. E. *J. Phys. Chem. A* **2001**, *105*, 1838.

(47) Hoffman, R. C.; Kaleuati, M. A.; Finlayson-Pitts, B. J. *J. Phys. Chem. A* **2003**, *107*, 7818.

(48) Spicer, C. W.; Chapman, E. G.; Finlayson-Pitts, B. J.; Plastridge, R. A.; Hubbe, J. M.; Dast, J. D.; Berkowitz, C. M. *Nature* **1998**, *394*, 353.

(49) Foster, K. L.; Plastridge, R. A.; Bottenheim, J. W.; Shepson, P. B.; Finlayson-Pitts, B. J.; Spicer, C. W. *Science* **2001**, *291*, 471.

(50) Spicer, C. W.; Plastridge, R. A.; Foster, K. L.; Finlayson-Pitts, B. J.; Bottenheim, J. W.; Grannas, A. M.; Shepson, P. B. *Atmos. Environ.* **2002**, *36*, 2721.